

Electronic supplementary information

Palladium(II) and platinum(II) complexes of glyoxalbis(N-aryl)osazone: molecular and electronic structures, anti-microbial activities and DNA-binding study

Sarat Chandra Patra,^{ab} Amit Saha Roy,^{ac} Saswati Banerjee,^d Ananya Banerjee,^e Krishna Das Saha,^d Ranjan Bhadra,^a Kausikisankar Pramanik^{*b} and Prasanta Ghosh^{*a}

^aDepartment of Chemistry, R. K. Mission Residential College, Narendrapur, Kolkata-103, India

^bDepartment of Chemistry, Jadavpur University, Kolkata-700032, India.

^cDepartment of Chemistry, New Alipore College, L Block, New Alipore, Kolkata-700053, India.

^dCancer Biology & Inflammatory Disorder, Indian Institute of Chemical Biology, 4, Raja S.C. Mallick Road, Kolkata 700032.

^eDepartment of Chemistry, Bijaygarh Jyotish Roy College, Jadavpur, Kolkata-700032, India.

*To whom correspondence should be addressed. Email: ghosh@pghosh.in

Phone: +91-33-2428-7347; Fax: +91-33-2477-3597

Table of Contents	
	Page No.
Materials and physical measurements	S2-S4
Crystallographic data for 2 and 4	S5
Molecular geometry of 2	S6
Cyclic voltammograms of 1 and 2 in DCM solvent	S6
Cyclic voltammograms of 1-4 in CH ₃ CN solvent	S7-S8
X-band EPR spectra of (a) [3] ⁻ and (b) [4] ⁻ in CH ₂ Cl ₂ solutions at 298 K	S8
EPR measurement parameters table	S9
Spin density plot of [3] ⁺	S9
Gas phase optimized geometries of 1 , 2 , 3 , 4 , [3] ⁻ and [4] ⁻	S9-10
Frontier molecular orbital composition (%) in the ground state for 1-4	S10
Transition types and dominant contributions of UV-vis-NIR absorption bands of 3	S10
FMO pictures of 1-4	S11
Absorption spectral change of (a) 1 and (b) 3 in presence of CT-DNA in buffer	S12
Fluorescence titration data of 1 and 3 on the displacement of CT-DNA	S12-S13
Comparative study of anti-leishmanial activity	S13
Anti-leishmanial activity of the compounds 1 and 3	S14
MIC values of 1 and 3 in bacterial system	S15
The antifungal activity (MIC) of 1 and 3	S15
Optimized coordinates of 1 , 2 , 3 , 4 , [3] ⁻ and [4] ⁻	S16- S21
References	S21-S23

Materials and physical measurements

Reagents or analytical grade materials were obtained from Sigma-Aldrich Corporation, India and used without further purification. Spectroscopic grade solvents were used for spectroscopic measurements. The C, H, N contents of the compounds were obtained from a Perkin-Elmer 2400 series II elemental analyzer. Infrared spectra of the samples were measured from 4000 to 400 cm^{-1} as KBr pellets at room temperature on a Perkin-Elmer FT-IR-Spectrophotometer Spectrum RX1. ^1H NMR spectral measurements were carried out on a Bruker DPX-300 MHz spectrometer with tetramethylsilane (TMS) as an internal reference. ESI mass spectra were recorded on a micro mass Q-TOF mass spectrometer. Electronic absorption spectra in solution at 298 K were measured on a Perkin-Elmer Lambda 750 UV-vis-NIR spectrophotometer in the range 3300–175 nm. Fluorescence quenching studies were recorded on a Perkin-Elmer LS 55 fluorescence spectrophotometer. The electro-analytical instrument, BASi Epsilon-EC has been used for cyclic voltammetric experiment containing a Pt working electrode and a Pt-wire auxiliary electrode. Tetrabutylammonium hexafluorophosphate (Bu_4NPF_6) was used as a supporting electrolyte, and the potentials are referenced to the Ag/AgCl electrode. The value of the Fc^+/Fc couple under similar experimental conditions is found to be 0.51 V vs Ag/AgCl. A BASi SEC-C thin layer quartz glass spectroelectrochemical cell kit (light path length of 1 mm) with platinum-gauze working electrode and SEC-C platinum counter electrode was used for spectroelectrochemical measurements. Changes in electronic absorption spectra in solution with fixed applied potentials were recorded on a PerkinElmer Lambda 750 spectrophotometer. The X-band electron paramagnetic resonance (EPR) spectra at 298 K were measured on a Magnettech GmbH MiniScope MS400 spectrometer (equipped with temperature controller TC H03), where the microwave frequency was measured with a frequency counter FC400. All the EPR spectra were simulated using Easy Spin software.¹

Biological studies

Roswell Park Memorial Institute medium-1640 (RPMI-1640), M-199 medium, fetal bovine serum (FBS), penicillin–streptomycin (PS) and HEPES were procured from Gibco BRL. Tissue culture plastic wares were acquired from NUNC (Roskilde, Denmark). The standard anti-leishmanial agent Miltefosine, MTT [(4,5-dimethyl-thiazol-2-yl)-2,5-diphenyl tetrazolium bromide] and DMSO were purchased from Sigma-Aldrich, USA. The culture media M-199 used for Leishmania was procured from Sigma-Aldrich, USA. Other culture media constituents FBS, penicillin, streptomycin and gentamycin, Trypan blue and cell cultured grade Na-bicarbonate were purchased from HiMedia, India. Another standard anti-leishmanial agent, SAG (sodium stibogluconate) was purchased from Albert-David, India. For bacterial and fungal culture Nutrient Broth and Czapek-Dox Broth/Agar, respectively, were purchased from Merck, India. Calf thymus DNA (CT-DNA, type I, 42% GC content) and analytical grade ethidium bromide (EB) [3, 8-di-amino-5-ethyl-6-phenylphenanthridium] were purchased from local supplier (SRL, India). All other reagents used were of highest purity grade available.

X-Ray crystallographic data collection and refinement of the structures

Single crystals of **2** (red) and **4** (red) were picked up with nylon loops and were mounted on a Bruker Kappa-CCD diffractometer equipped with a Mo-target rotating anode X-ray source and a graphite monochromator (Mo-K α , $\lambda = 0.71073 \text{ \AA}$). Final cell constants were obtained from least squares fits of all measured reflections. Structures were readily solved by Patterson method and subsequent difference Fourier techniques. The crystallographic data are listed in Table 1. ShelXS97^{2a} and ShelXL97^{2b} were used for the structure solution and refinement. All the non-hydrogen atoms were refined anisotropically. Hydrogen atoms were placed at the calculated positions and refined as riding atoms with isotropic displacement parameters.

Density functional theory (DFT) calculations

All calculations reported in this article were done with the Gaussian 03W³ program package supported by GaussView 4.1. The DFT⁴ and TD DFT⁵ calculations were performed at the level of Becke three parameter hybrid functional with the non-local correlation functional of Lee-Yang-Parr (B3LYP).⁶ Gas-phase geometries of *cis*-[Pd(L^{NHPh}H₂)Cl₂] (**1**), *cis*-[Pd(L^{NH(CIPh)}H₂)Cl₂] (**2**), *cis*-[Pt(L^{NHPh}H₂)Cl₂] (**3**), *cis*-[Pt(L^{NHAr}H₂)Cl₂] (**4**), with singlet spin state and *cis*-[Pt(L^{NHPh}H₂)Cl₂]⁻ (**3**⁻), *cis*-[Pt(L^{NHAr}H₂)Cl₂]⁻ (**4**⁻) with doublet spin state were optimized using Pulay's Direct Inversion⁷ in the Iterative Subspace (DIIS), 'tight' convergent SCF procedure⁸ ignoring symmetry. In all calculations, a LANL2DZ basis set along with the corresponding effective core potential (ECP) was used for platinum metal.⁹ Valence double zeta basis set, 6-31G¹⁰ for H was used. For C, N and Cl non-hydrogen atoms valence double zeta with diffuse and polarization functions, 6-31++G^{**11} as basis set was employed for all calculations. The percentage contributions of metal, chloride and osazone ligand to the frontier orbitals were calculated using GaussSum programme package.¹² The sixty lowest singlet excitation energies on the optimized geometry of **3** were calculated by TD DFT method in CH₂Cl₂ solvent using PCPM model.¹³ The nature of transitions were calculated by adding the probability of same type among alpha and beta molecular orbital.

Table S1 Crystallographic data for **2** and **4**

	2	4
formula	C ₁₄ H ₁₂ Cl ₄ N ₄ Pd	C ₁₄ H ₁₂ Cl ₄ N ₄ Pt
CCDC no.	1534727	1534728
Fw	484.48	572.98
cryst colour	red	orange
cryst syst	Orthorhombic	Orthorhombic
space group	<i>Pnma</i>	<i>Cmc2(1)</i>
<i>a</i> (Å)	7.35830(10)	28.6797(10)
<i>b</i> (Å)	29.4166(5)	7.9654(3)
<i>c</i> (Å)	7.90080(10)	7.5874(3)
β (deg)	90.00	90.00
<i>V</i> (Å ³)	1710.18(4)	1733.31(11)
<i>Z</i>	4	4
<i>T</i> (K)	273(2)	293(2)
calcd (g cm ⁻³)	1.882	2.196
reflns collected/ $2\theta_{\max}$	17080/56.32	12668/55.24
unique reflns/ <i>R</i> _{int}	2076/0.0278	2049/0.0356
reflns [<i>I</i> > 2σ(<i>I</i>)]	1879	1991
λ (Å) / μ (mm ⁻¹)	0.71073/1.712	0.71073/8.714
F(000)	952	1080
<i>R</i> 1 ^a [<i>I</i> > 2σ(<i>I</i>)] / GOF ^b	0.0379/1.280	0.0385/1.064
<i>R</i> 1 ^a (all data)	0.0426	0.0393
w <i>R</i> 2 ^c [<i>I</i> > 2σ(<i>I</i>)]	0.1215	0.1107
no. of param./ restr.	130 / 0	106 / 1
residual density (eÅ ⁻³)	0.952	1.244
^a <i>R</i> 1 = $\sum F_o - F_c / \sum F_o $. ^b GOF = $\{\sum [w(F_o^2 - F_c^2)^2] / (n-p)\}^{1/2}$. ^c w <i>R</i> 2 = $[\sum [w(F_o^2 - F_c^2)^2] / \sum [w(F_o^2)^2]]^{1/2}$ where $w = 1/[\sigma^2(F_o^2) + (aP)^2 + bP]$, $P = (F_o^2 + 2F_c^2)/3$.		

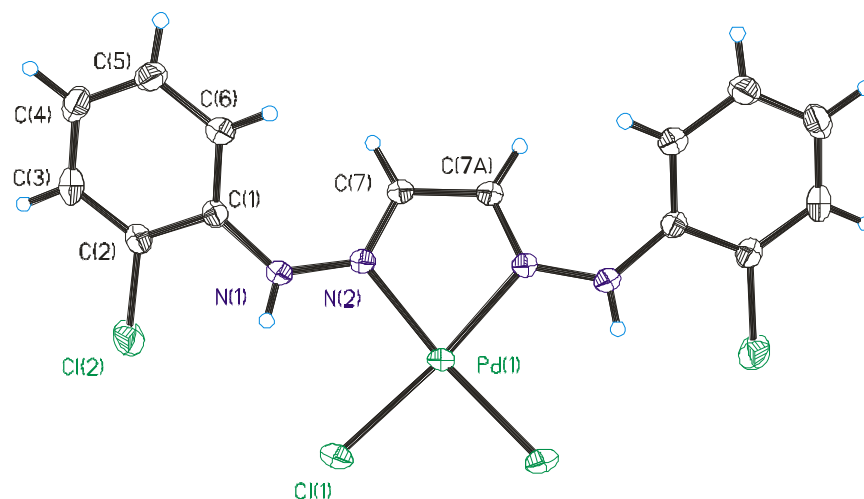


Fig. S1 Molecular geometry of **2** (40% thermal ellipsoid).

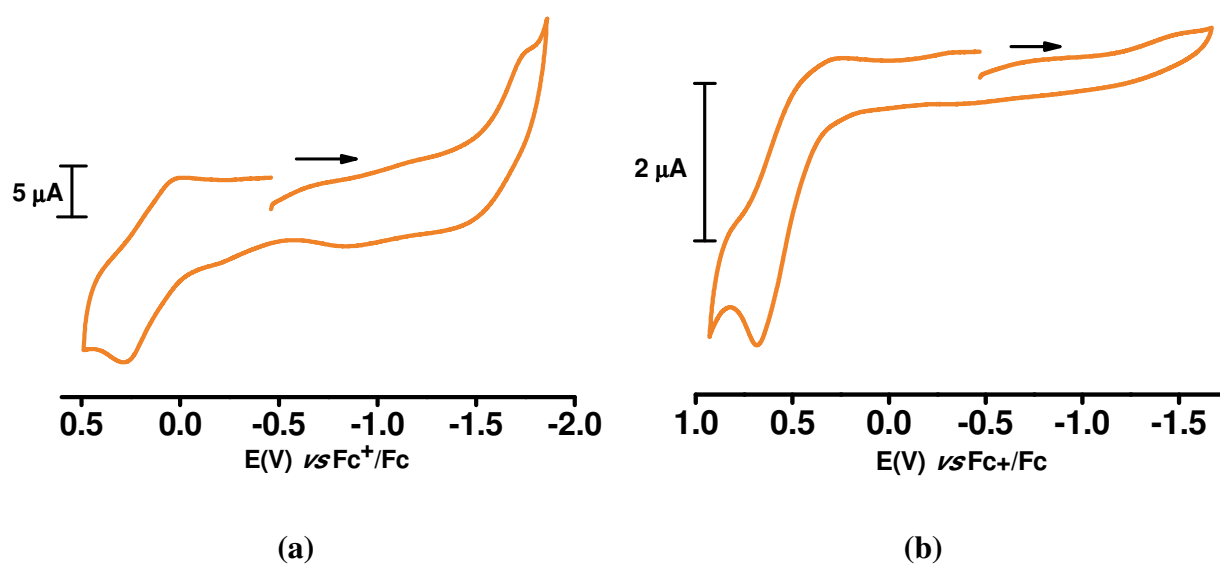
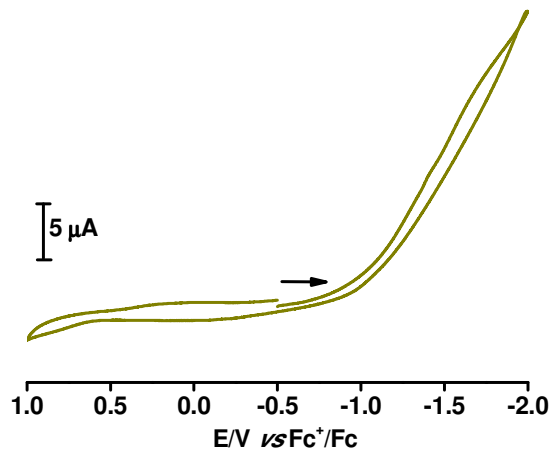
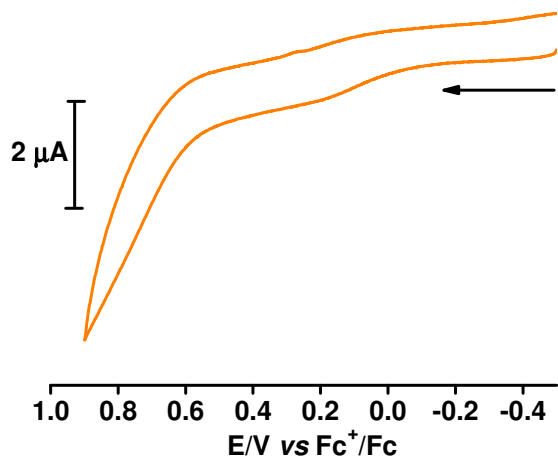
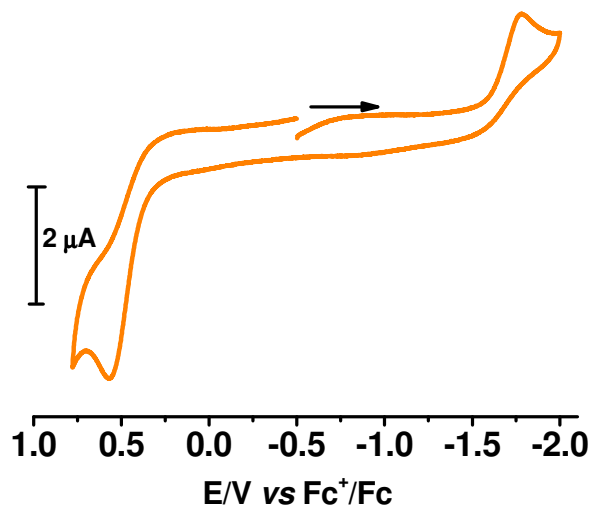
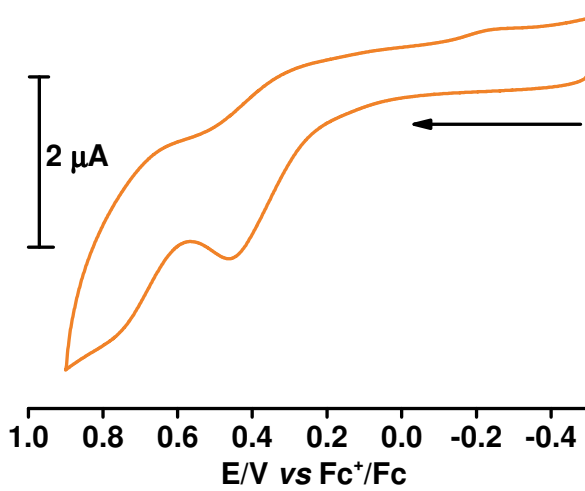


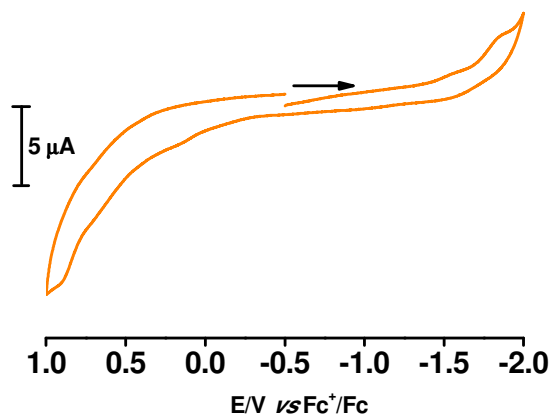
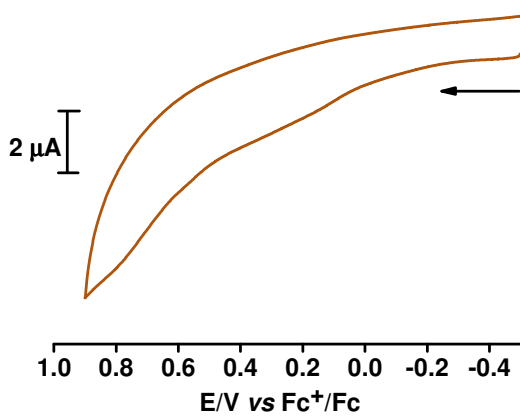
Fig. S2 Cyclic voltammograms of (a) $[\text{Pd}(\text{L}^{\text{NHPH}_2})\text{Cl}_2]$ (**1**) and (b) $[\text{Pd}(\text{L}^{\text{NH}(\text{CIPh})\text{H}_2})\text{Cl}_2]$ (**2**) (scan rate: 100) in CH_2Cl_2 solvent at 298K. Conditions: 0.20 M $[\text{N}(\text{n-Bu})_4]\text{PF}_6$ supporting electrolyte; platinum working electrode.



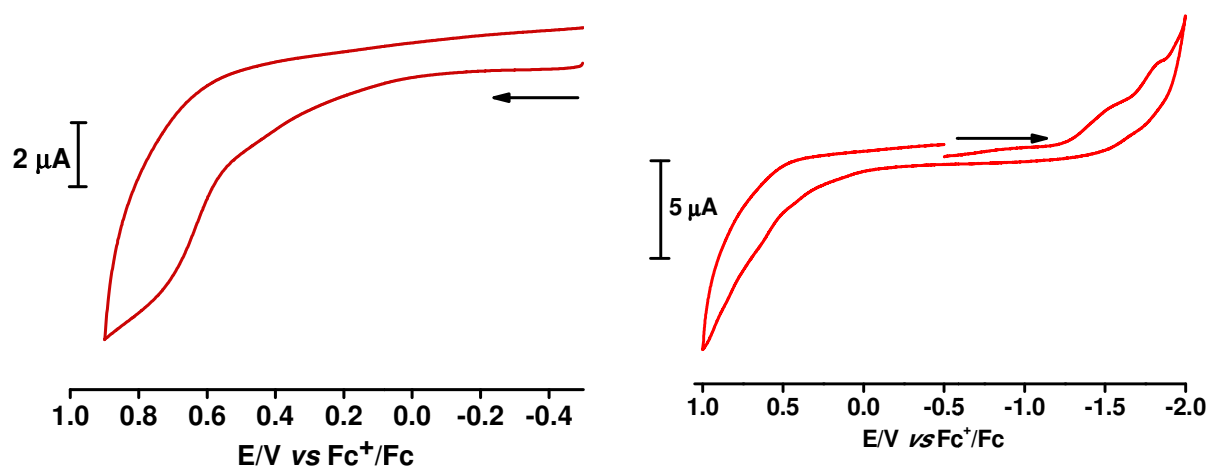
(1)



(2)



(3)



(4)

Fig. S3 Cyclic voltammograms of $[\text{Pd}(\text{L}^{\text{NHPH}}\text{H}_2)\text{Cl}_2]$ (1), $[\text{Pd}(\text{L}^{\text{NH(CIPh)}}\text{H}_2)\text{Cl}_2]$ (2), $[\text{Pt}(\text{L}^{\text{NHPH}}\text{H}_2)\text{Cl}_2]$ (3) and $[\text{Pt}(\text{L}^{\text{NH(CIPh)}}\text{H}_2)\text{Cl}_2]$ (4) (scan rate:100) in CH_3CN solvent at 298K. Left: Anodic scan only, Right: Full range scan (-2 to +2 V). Conditions: 0.20 M $[\text{N}(\text{n-Bu})_4]\text{PF}_6$ supporting electrolyte; platinum working electrode.

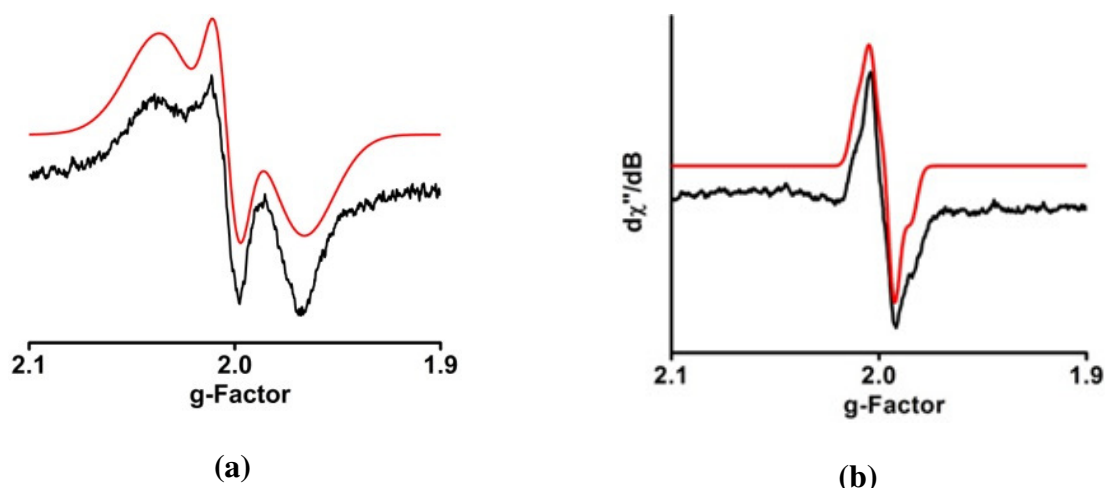
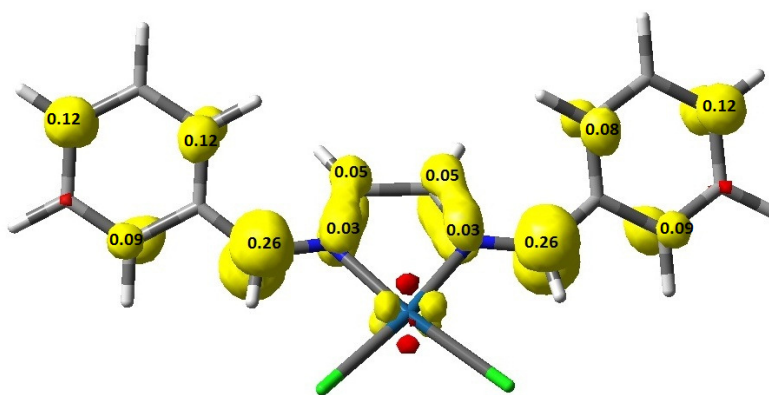
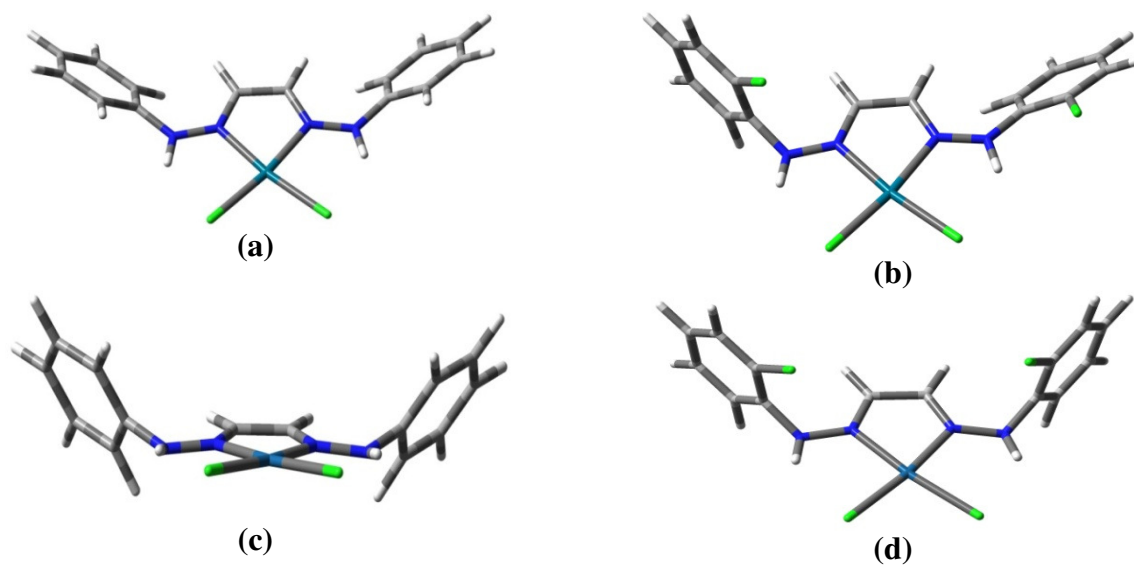


Fig. S4 X-band EPR spectra of (a) $[\mathbf{3}]^-$ and (b) $[\mathbf{4}]^-$ in CH_2Cl_2 at 298 K. (black = experimental, red = simulated).

Table S2 EPR measurement parameters

Complexes	Conditions	Temp	Mod.	B ₀	B ₀	Frequency	Sweep
		(K)	Amp.	Field	Sweep	(GHz)	Time
			(G)	(mT)	(mT)		(s)
[3] ⁺	CH ₂ Cl ₂ solution	298	0.15	336.83	199.74	9.47320	30
[4] ⁺		298	0.18	338.77	149.95	9.47340	30

**Fig. S5** Spin density plots of [3]⁺; values from Mulliken spin population analyses (isovalue = 0.004).

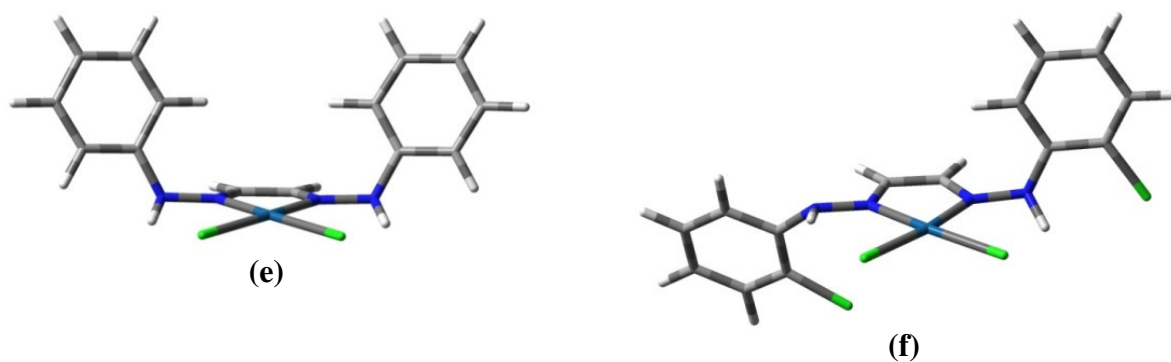


Fig. S6 Gas phase optimized geometries of (a) **1**, (b) **2**, (c) **3**, (d) **4**, (e) $[3]^-$ and (f) $[4]^-$.

Table S3 Frontier molecular orbital composition (%) in the ground state for **1-4**

			% Contribution			
			MCl ₂		Osazone Ligand	Major participation of orbitals
MO number	MO descriptions	Energy (eV)	M	Cl		
1						
90	LUMO	-2.86	5	1	94	π^* (Osazone)
89	HOMO	-6.02	3	4	93	π (Osazone)
2						
106	LUMO	-2.93	11	5	84	π^* (Osazone)
105	HOMO	-6.22	8	11	81	π (Osazone)
3						
90	LUMO	-2.87	8	1	91	π^* (Osazone)
89	HOMO	-6.09	18	18	64	π (Osazone) + d_{Pt} + p_{Cl}
4						
106	LUMO	-2.96	10	2	88	π^* (Osazone)
105	HOMO	-6.15	28	34	38	π (Osazone) + d_{Pt} + p_{Cl}

Table S4 Excitation energies (λ/nm), oscillator strengths (f), significant contributions (>10%), transition types and dominant contributions of UV-vis-NIR absorption bands of **3** obtained from TD DFT calculations

λ_{calc}/nm	f	λ_{exp}/nm	significant contributions (>10%)	transition types	dominant contributions
472.00	0.1016	452	HOMO-3 \rightarrow LUMO (39%)	π_L (92%) \rightarrow π^*_L (64%) + d_{Pt} (36%)	LMMLCT
405.25	0.0514	354	HOMO-5 \rightarrow LUMO (46%)	π_L (95%) \rightarrow π^*_L (64%) + d_{Pt} (36%)	LMMLCT
284.90	0.0378	301	HOMO-3 \rightarrow LUMO + 1 (17%)	π_L (92%) \rightarrow π^*_L (89%)	$\pi \rightarrow \pi^*$

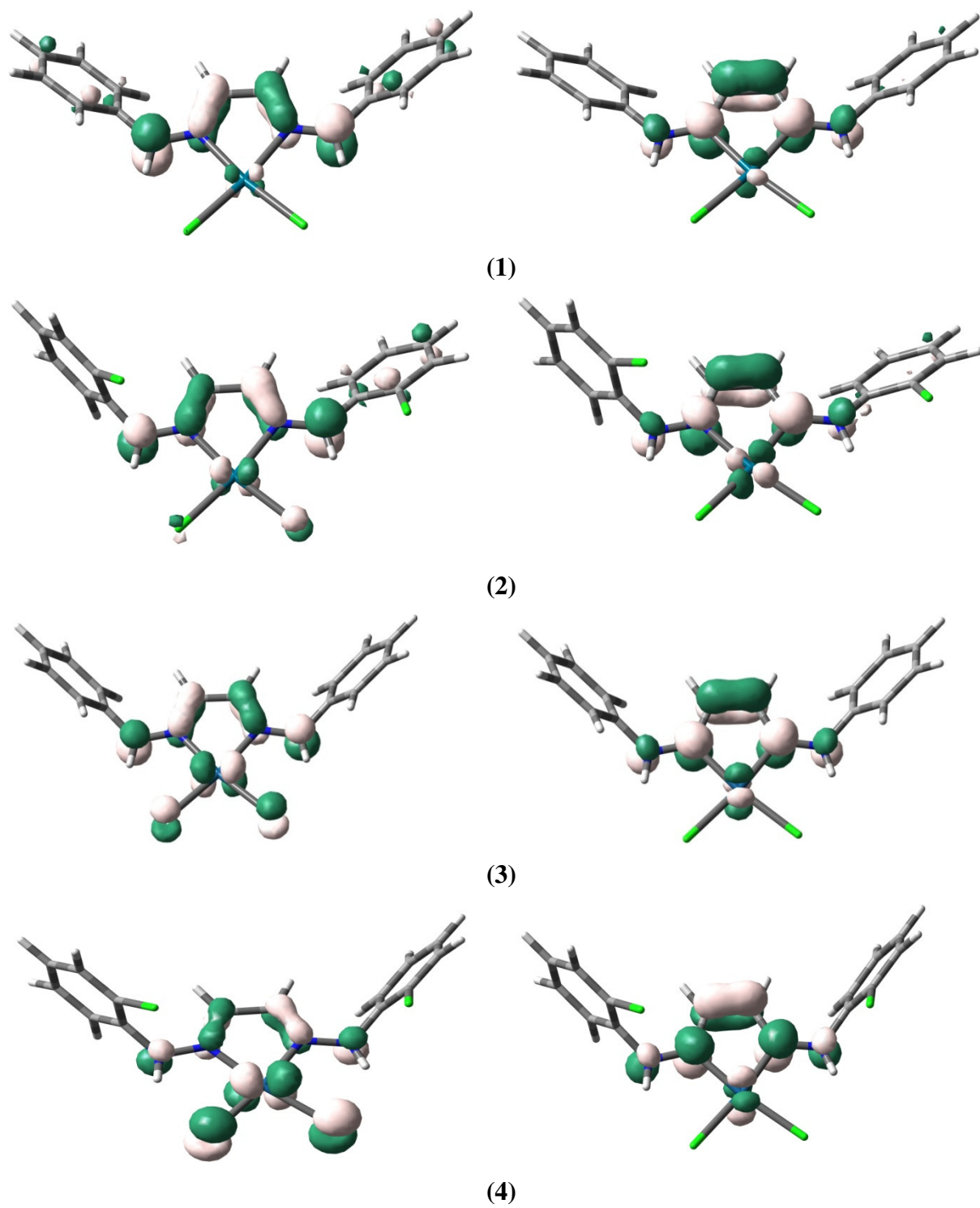


Fig. S7. FMOs of 1-4; HOMOs (left column) and LUMOs (right column) (isovalues = 0.06).

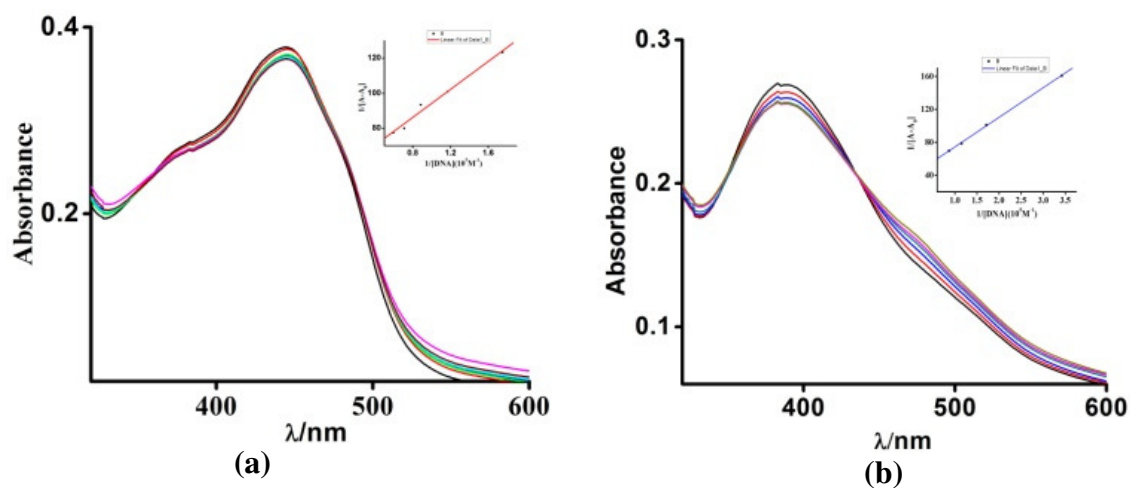


Fig. S8 Absorption spectra of (a) **1** ($2.89 \times 10^{-5} \text{ mol L}^{-1}$) and (b) **3** ($2.29 \times 10^{-5} \text{ mol L}^{-1}$) in presence of CT-DNA in buffer at 298 K. (The insets show the Benesi-Hildebrand plots of binding).

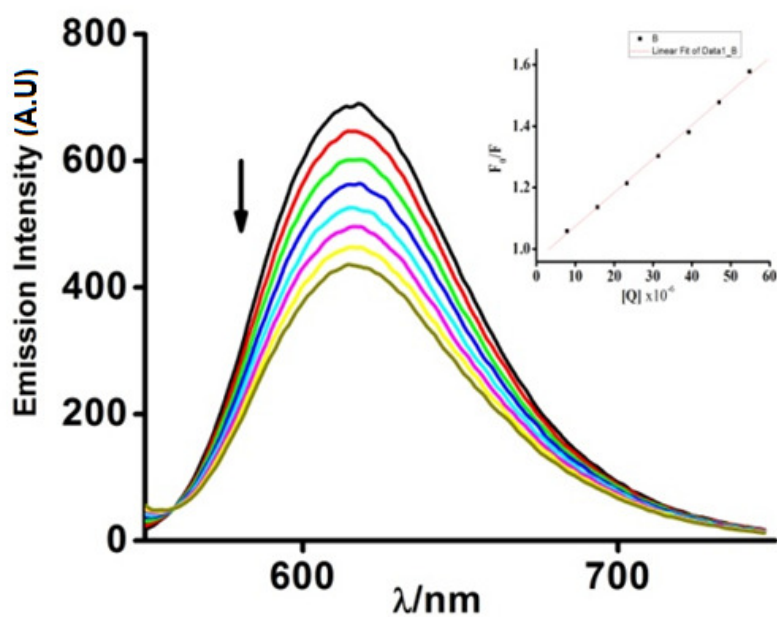


Fig. S9 Fluorescence titration data on the displacement of CT-DNA bound ethidium bromide by **1** (Inset shows the Stern-Volmer plot of quenching study).

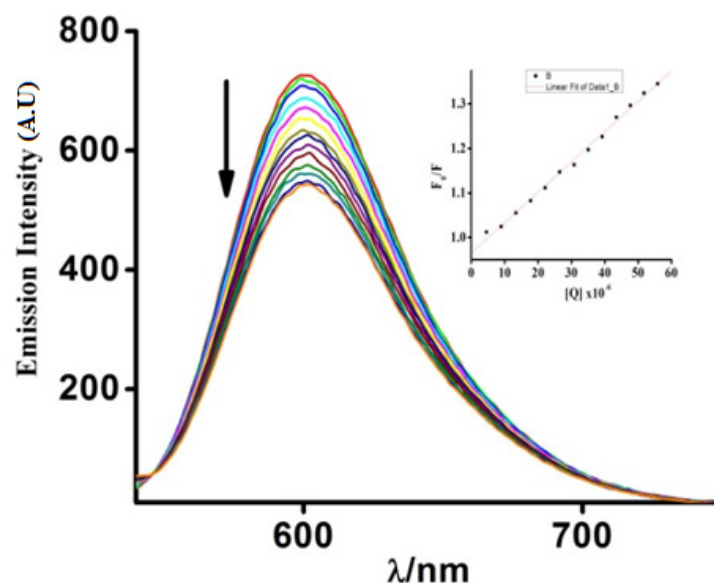


Fig. S10 Fluorescence titration data on the displacement of CT-DNA bound ethidium bromide by **3** (Inset shows the Stern-Volmer plot of quenching study).

Table S5 Comparative study of IC₅₀ values (μM) among some previously reported⁷ palladium (II) and platinum (II) nitrofurylthiosemicarbazone complexes by Gambino et al. and the compounds reported in this article.

Compounds	Studied promastigotes	IC ₅₀ in μM after 48 hrs of incubation	Compounds	Studied promastigotes	IC ₅₀ in μM after 48 hrs of incubation
This paper			Reference 8		
$L^{NHPh}H_2$	<i>Leishmania donavani</i>	>30	[PdCl ₂ (HL1)]	<i>T. cruzi</i> <i>Tulahuen 2</i>	2.4 ± 0.1
$L^{NH(CIPh)}H_2$		>30	[PdCl ₂ (HL2)]		4.3 ± 0.1
1		25.00 ± 0.06	[PdCl ₂ (HL3)]		5.9 ± 0.1
2		>30	[PdCl ₂ (HL4)]		>25
3		19.69 ± 0.13	[PdCl ₂ (HL5)]		6.4 ± 0.1
4		>30	[PdCl ₂ (HL6)]		2.7 ± 0.1
Miltefosine		15.14 ± 0.81	[PdCl ₂ (HL7)]		2.4 ± 0.1
Reference 8			[PdCl ₂ (HL8)]		>>25
L1	<i>T. cruzi</i> <i>Tulahuen 2</i>	2.7 ± 0.1	[PtCl ₂ (HL1)]	6.4 ± 0.1	
L2		5.0 ± 0.1	[PtCl ₂ (HL2)]	13.1 ± 0.1	
L3		4.9 ± 0.1	[PtCl ₂ (HL3)]	27.5 ± 0.1	
L4		>25	[PtCl ₂ (HL4)]	15.0 ± 0.1	
L5		3.5 ± 0.1	[PtCl ₂ (HL5)]	8.6 ± 0.1	
L6		4.5 ± 0.1	[PtCl ₂ (HL6)]	10.0 ± 0.1	
L7		4.1 ± 0.1	[PtCl ₂ (HL7)]	13.7 ± 0.1	
L8		3.6 ± 0.1	[PtCl ₂ (HL8)]	>25	
			Nifurtimox	6.1 ± 0.1	

Table S6 Anti-leishmanial activity of the compounds **1** and **3** (at a dose 30 μ M)

Name of compounds	Activity against UR-6	Cell morphology (in 10 μ l)		Cell motility (in 10 μ l)		Viable cell count (cells/ml)	
		24hrs	72hrs	24hrs	72hrs	24hrs	72hrs
Control (without SAG)	-	Morphologically unchanged	Morphologically unchanged	Highly motile	Highly motile	3x10 ⁵	8x10 ⁵
Control (without SAG but with 10% DMSO)	-	Morphologically unchanged	Morphologically unchanged	Highly motile	Highly motile	3.1 x10 ⁵	7.8x10 ⁵
SAG (Standard anti-leishmanial drug) (10 μ M)	+	20% cells with changed morphology and the rest remaining unchanged (80%)	40% cells with changed morphology and the rest remaining unchanged (60%)	70% non motile	80% non motile	4x10 ³	1x10 ³
1 (30 μ M)	+	Morphology totally changed in 80%.	Morphology totally changed in 90%	70% non motile	90% non motile	1x10 ²	7x10 ²
3 (30 μ M)	+	Morphology totally changed in 90%.	Morphology totally changed in 99%	95% non motile	99% non motile	5x10	2.2x10
Control (without SAG)	Against AG 83 -	Morphologically unchanged	Morphologically unchanged	Highly motile	Highly motile	3.6x10 ⁵	6.25x10 ⁵
Control (without SAG but with 10% DMSO)	-	Morphologically unchanged	Morphologically unchanged	Highly motile	Highly motile	2.7 x10 ⁵	4.75x10 ⁵
SAG (Standard anti-leishmanial drug) (10 μ M)	+	30%cells with changed morphology and the rest remaining unchanged 70(%)	50% cells with changed morphology and the rest remaining unchanged (50%)	75% non motile	90% non motile	2.25x10 ⁴	1.5x10 ⁴
1 (30 μ M)	+	No such distinguishable change in Morphology. Dead cells have become little elongated	No such distinguishable change in Morphology. Dead cells have become little elongated	80% non motile	95% non motile	2x10 ³	1.25x10 ³
3 (30 μ M)	+	No such distinguishable change in Morphology. Dead cells have become little elongated	No such distinguishable change in Morphology. Dead cells have become little elongated	90% non motile	98% non motile	4.5x10 ²	2.5x10 ²

Table S7 Determination of minimum inhibitory concentration (MIC) of **1** and **3** in bacterial system

Name of the organisms	MIC value in μM	MIC value in μM	MIC value in μM	MIC value in μM	10% DMSO
	1	3	Streptomycin	Tetracycline	
<i>Bacillus subtilis</i>	>100	>100	1.4	2.2	—
<i>Staphylococcus aureus</i> ATCC25923	>100	>100	1.7	1.8	—
<i>Klebsiella pneumoniae</i>	>100	>100	1.5	1	—
<i>Escherichia coli</i>	>100	>100	1.4	2.2	—
<i>Salmonella typhi</i> ATCC 34	>100	>100	8.6	1.8	—
<i>Pseudomonas aeruginosa</i> ATCC27853	>100	>100	1.2	6.8	—
<i>Vibrio cholera</i>	>100	>100	10.3	1.8	—
<i>Salmonella typhimurium</i>	>100	>100	0.7	1.6	—
<i>Enterococcus faecalis</i>	>100	>100	1.2	1.8	—
<i>Shigella dysenteriae</i>	>100	>100	1.5	1.6	—
<i>Proteus vulgaris</i>	>100	>100	1.4	2.2	—
—sign indicates no inhibition					

Table S8 The antifungal activity (MIC) of **1** and **3**

Name of organisms	MIC value in μM			10% DMSO
	1	3	Nystatin	
<i>Aspergillus oryzae</i>	>100	108	8.6	—
<i>Aspergillus niger</i>	>100	>100	4.3	—
<i>Saccharomyces cerevisiae</i>	>100	>100	8.6	—
<i>Penicillium chrysogenum</i>	>100	>100	108	—

Table S9 Optimized coordinates of **1**

Center number	Atomic number	Atomic type	Coordinates (Angstroms)		
			X	Y	Z
1	7	0	1.168845	0.649005	1.350385
2	7	0	3.074175	-1.156236	0.945605
3	6	0	2.280270	1.054233	0.790182
4	1	0	2.429896	2.084447	0.484870
5	6	0	3.313738	0.074345	0.569822
6	1	0	4.247061	0.362186	0.097621
7	17	0	-1.056681	-1.391072	2.460706
8	17	0	1.392432	-3.710852	1.943322
9	7	0	3.916443	-2.194012	0.841282
10	1	0	3.428860	-3.069824	1.042351
11	7	0	0.108571	1.411985	1.646368
12	1	0	-0.687075	0.830165	1.917719
13	6	0	-1.299007	3.210034	0.870845
14	6	0	-0.066072	2.790254	1.396492
15	6	0	0.909189	3.744261	1.731960
16	6	0	0.653737	5.099983	1.517995
17	6	0	-0.571559	5.519261	0.990556
18	6	0	-1.549038	4.569089	0.678700
19	1	0	-2.050924	2.468089	0.615230
20	1	0	1.840280	3.436127	2.196597
21	1	0	1.411075	5.832344	1.784904
22	1	0	-0.765312	6.576279	0.831842
23	1	0	-2.507163	4.883486	0.273857
24	6	0	5.489604	-3.274355	-0.635440
25	6	0	6.762056	-3.379028	-1.198081
26	6	0	7.742194	-2.423196	-0.913296
27	6	0	7.446133	-1.370944	-0.041243
28	6	0	6.182448	-1.266001	0.542886
29	6	0	5.192190	-2.214052	0.236198
30	1	0	4.721072	-4.007079	-0.867203
31	1	0	6.982602	-4.204677	-1.869203
32	1	0	8.729493	-2.501861	-1.359478
33	1	0	8.208370	-0.636274	0.204529
34	1	0	5.983593	-0.480054	1.264413
35	46	0	1.151475	-1.403683	1.709613

Table S10 Optimized coordinates of **2**

Center number	Atomic number	Atomic type	Coordinates (Angstroms)		
			X	Y	Z
1	46	0	1.267981	-1.2518	2.241993
2	7	0	1.177922	0.629537	1.339146
3	7	0	3.132822	-1.16058	1.33274
4	6	0	2.258645	0.91686	0.659611
5	1	0	2.358508	1.838501	0.095134
6	6	0	3.319603	-0.06063	0.655441
7	1	0	4.241431	0.126044	0.110678
8	17	0	-0.88178	-1.08025	3.119221
9	17	0	1.63902	-3.38506	3.09462
10	7	0	4.060217	-2.13078	1.48138
11	1	0	3.625569	-2.9714	1.870556
12	7	0	0.084782	1.396246	1.433832
13	1	0	-0.6723	0.899176	1.911276
14	6	0	-1.2678	3.217385	0.568363
15	6	0	-0.04368	2.753525	1.091984
16	6	0	0.981111	3.68924	1.31981
17	6	0	0.797112	5.036187	1.014443
18	6	0	-0.42075	5.479864	0.490239
19	6	0	-1.45644	4.568855	0.278179
20	1	0	1.911104	3.360626	1.771938
21	1	0	1.601066	5.741466	1.204896
22	1	0	-0.56979	6.529142	0.253161
23	1	0	-2.41188	4.894481	-0.12046
24	6	0	5.110051	-2.8098	-0.66157
25	6	0	6.247447	-2.91292	-1.46583
26	6	0	7.472146	-2.43018	-0.99888
27	6	0	7.567351	-1.8504	0.269329
28	6	0	6.428876	-1.75388	1.070838
29	6	0	5.191521	-2.23018	0.618554
30	1	0	6.167842	-3.37253	-2.44573
31	1	0	8.353075	-2.51571	-1.6291
32	1	0	8.521621	-1.48347	0.635666
33	1	0	6.478072	-1.32199	2.066266
34	17	0	-2.58016	2.093252	0.290835
35	17	0	3.584391	-3.42506	-1.25003

Table S11 Optimized coordinates of **3**

Center number	Atomic number	Atomic type	Coordinates (Angstroms)		
			X	Y	Z
1	78	0	1.233200	-1.377852	1.938873
2	7	0	1.260092	0.641015	1.613700
3	7	0	3.132732	-1.132155	1.225988
4	6	0	2.368221	1.070895	1.057991
5	1	0	2.505129	2.109790	0.781366
6	6	0	3.398149	0.094150	0.843543
7	1	0	4.349214	0.361510	0.397529
8	17	0	-1.009776	-1.400318	2.646754
9	17	0	1.435557	-3.710483	2.149585
10	7	0	4.005153	-2.168337	1.163762
11	1	0	3.499679	-3.045065	1.306477
12	7	0	0.206454	1.421036	1.949199
13	1	0	-0.603645	0.832525	2.153836
14	6	0	-1.113197	3.013045	0.667813
15	6	0	0.001758	2.743763	1.474406
16	6	0	0.854200	3.788196	1.863992
17	6	0	0.601813	5.088838	1.424326
18	6	0	-0.509680	5.360022	0.618996
19	6	0	-1.370202	4.321448	0.251690
20	1	0	-1.770164	2.199023	0.372894
21	1	0	1.684779	3.585944	2.534233
22	1	0	1.262574	5.895343	1.730903
23	1	0	-0.707963	6.375659	0.288065
24	1	0	-2.239223	4.525244	-0.367994
25	6	0	5.236223	-3.039271	-0.751022
26	6	0	6.401182	-3.098911	-1.519791
27	6	0	7.493092	-2.283265	-1.209008
28	6	0	7.425158	-1.418535	-0.111203
29	6	0	6.273269	-1.368751	0.676036
30	6	0	5.170659	-2.171602	0.348241
31	1	0	4.378302	-3.659895	-0.995976
32	1	0	6.449961	-3.777548	-2.367045
33	1	0	8.395403	-2.327190	-1.812649
34	1	0	8.278564	-0.797313	0.147199
35	1	0	6.236305	-0.738585	1.560195

Table S12 Optimized coordinates of **4**

Center number	Atomic number	Atomic type	Coordinates (Angstroms)		
			X	Y	Z
1	78	0	1.325952	-1.207779	2.450371
2	7	0	1.320552	0.735065	1.827972
3	7	0	3.130083	-1.101883	1.502121
4	6	0	2.373175	1.074684	1.126173
5	1	0	2.486608	2.071760	0.713735
6	6	0	3.373489	0.058932	0.946305
7	1	0	4.286516	0.245196	0.390610
8	17	0	-0.805792	-1.069172	3.428288
9	17	0	1.561003	-3.479820	2.995307
10	7	0	4.005847	-2.142130	1.490720
11	1	0	3.520867	-2.997660	1.773694
12	7	0	0.320322	1.594366	2.150804
13	1	0	-0.482813	1.068239	2.505505
14	6	0	-0.490382	2.815718	0.145264
15	6	0	0.115480	2.800161	1.416142
16	6	0	0.509427	4.013371	1.994995
17	6	0	0.307797	5.222430	1.327321
18	6	0	-0.293657	5.222749	0.065805
19	6	0	-0.695425	4.023085	-0.526343
20	1	0	0.963559	3.984918	2.981219
21	1	0	0.612221	6.155938	1.791378
22	1	0	-0.459282	6.158223	-0.461490
23	1	0	-1.172104	4.016412	-1.501305
24	6	0	4.823680	-2.660092	-0.795288
25	6	0	5.879010	-2.740411	-1.706903
26	6	0	7.165370	-2.365786	-1.312115
27	6	0	7.403700	-1.918111	-0.009617
28	6	0	6.346900	-1.845231	0.899097
29	6	0	5.049266	-2.212064	0.520085
30	1	0	5.687929	-3.097929	-2.713664
31	1	0	7.981806	-2.432368	-2.025962
32	1	0	8.405879	-1.636324	0.299761
33	1	0	6.507060	-1.516996	1.922035
34	17	0	-1.008602	1.322487	-0.598131
35	17	0	3.219245	-3.136198	-1.295370

Table S13 Optimized coordinates of [3]⁻

Center number	Atomic number	Atomic type	Coordinates (Angstroms)		
			X	Y	Z
1	78	0	1.071240	-1.290535	0.860808
2	7	0	0.755480	0.482766	-0.055422
3	7	0	2.584399	-1.276506	-0.477739
4	6	0	1.558302	0.710524	-1.116071
5	1	0	1.408800	1.591969	-1.730991
6	6	0	2.550820	-0.241970	-1.343625
7	1	0	3.269056	-0.190220	-2.155390
8	17	0	-0.874768	-1.081631	2.255335
9	17	0	1.628795	-3.477237	1.684597
10	7	0	3.585991	-2.238754	-0.623930
11	1	0	3.198093	-3.126880	-0.304806
12	7	0	-0.236646	1.417937	0.247389
13	1	0	-1.011707	0.906648	0.670632
14	6	0	-0.940163	3.342504	1.525862
15	6	0	0.108723	2.557939	1.007163
16	6	0	1.433527	2.971763	1.220316
17	6	0	1.693700	4.148638	1.928026
18	6	0	0.653465	4.931043	2.436799
19	6	0	-0.667807	4.511003	2.233024
20	1	0	-1.968060	3.021143	1.371827
21	1	0	2.250794	2.362661	0.851844
22	1	0	2.727458	4.447051	2.090821
23	1	0	0.864958	5.843455	2.988946
24	1	0	-1.494057	5.096411	2.631573
25	6	0	5.760166	-3.069157	0.025034
26	6	0	7.047983	-2.877594	0.519709
27	6	0	7.469394	-1.609913	0.942754
28	6	0	6.568924	-0.543561	0.870990
29	6	0	5.272687	-0.723863	0.380408
30	6	0	4.855524	-1.992242	-0.054164
31	1	0	5.438746	-4.056103	-0.300880
32	1	0	7.726841	-3.726058	0.578872
33	1	0	8.475020	-1.461322	1.328435
34	1	0	6.869599	0.445161	1.211928
35	1	0	4.577700	0.107297	0.352831

Table S14 Optimized coordinates of [4]⁻

Center number	Atomic number	Atomic type	Coordinates (Angstroms)		
			X	Y	Z
1	78	0	1.860231	-0.877379	1.746194
2	7	0	1.901891	1.090206	1.275606
3	7	0	2.826012	-0.928664	-0.033045
4	6	0	2.525245	1.382092	0.114641
5	1	0	2.600072	2.406673	-0.234650
6	6	0	3.017126	0.287698	-0.590860
7	1	0	3.536070	0.364864	-1.540827
8	17	0	0.737826	-0.471587	3.845040
9	17	0	1.882838	-3.244352	2.026277
10	7	0	3.406526	-2.024566	-0.675608
11	1	0	2.753164	-2.804553	-0.667222
12	7	0	1.417778	2.104161	2.086723
13	1	0	1.154955	1.686755	2.984302
14	6	0	-0.406462	3.021746	0.575311
15	6	0	0.537665	3.111383	1.622944
16	6	0	0.617191	4.341539	2.311135
17	6	0	-0.182749	5.430401	1.980493
18	6	0	-1.074801	5.336365	0.906196
19	6	0	-1.177911	4.131598	0.211364
20	1	0	1.349310	4.413161	3.111282
21	1	0	-0.090999	6.356994	2.542074
22	1	0	-1.689884	6.184055	0.615368
23	1	0	-1.886474	4.023502	-0.604632
24	6	0	5.255635	-3.613238	-0.766714
25	6	0	6.559445	-3.996378	-0.464289
26	6	0	7.364255	-3.168268	0.322761
27	6	0	6.836359	-1.965222	0.801435
28	6	0	5.528605	-1.588845	0.501023
29	6	0	4.703631	-2.405107	-0.294656
30	1	0	6.934141	-4.941594	-0.845997
31	1	0	8.381812	-3.466574	0.561115
32	1	0	7.441041	-1.316080	1.430370
33	1	0	5.114977	-0.669363	0.898398
34	17	0	-0.732662	1.516175	-0.260989
35	17	0	4.272835	-4.683817	-1.772040

References

1. (a) S. Stoll, Chapter Six- CW-EPR Spectral Simulations: Solid State. *Methods Enzymol.* 2015, **563**, 121-142; (b) S. Stoll, A. Schweiger, EasySpin, a comprehensive software package for spectral simulation and analysis in *EPR. J. Magn. Reson.* 2006, **178**, 42-55.
2. (a) G. M. Sheldrick, ShelXS97, UniversitätGöttingen, Göttingen, Germany, 1997; (b) G. M. Sheldrick, ShelXL97, UniversitätGöttingen, Göttingen, Germany, 1997.
3. M. J. Frisch, G. W. Trucks, H. B. Schlegel, G. E. Scuseria, M. A. Robb, J. R. Cheeseman, J. A. Montgomery Jr., T. Vreven, K. N. Kudin, J. C. Burant, J. M. Millam, S. S. Iyengar, J. Tomasi, V. Barone, B. Mennucci, M. Cossi, G. Scalmani, N. Rega, G. A. Petersson, H. Nakatsuji, M. Hada, M. Ehara, K. Toyota, R. Fukuda, J. Hasegawa, M. Ishida, T. Nakajima, Y. Honda, O. Kitao, H. Nakai, M. Klene, X. Li, J. E. Knox, H. P. Hratchian, J. B. Cross, V. Bakken, C. Adamo, J. Jaramillo, R. Gomperts, R. E. Stratmann, O. Yazyev, J. A. Austin, R. Cammi, C. Pomelli, J. W. Ochterski, P. Y. Ayala, K. Morokuma, G. A. Voth, P. Salvador, J. J. Dannenberg, V. G. Zakrzewski, S. Dapprich, A. D. Daniels, M. C. Strain, O. Farkas, D. K. Malick, A. D. Rabuck, K. Raghavachari, J. B. Foresman, J. V. Ortiz, Q. Cui, A. G. Baboul, S. Clifford, J. Cioslowski, B. B. Stefanov, G. Liu, A. Liashenko, P. Piskorz, I. Komaromi, R. L. Martin, D. J. Fox, T. Keith, M. A. Al-Laham, C. Y. Peng, A. Nanayakkara, M. Challacombe, P. M. W. Gill, B. Johnson, W. Chen, M. W. Wong, C. Gonzalez and J. A. Pople, Gaussian 03, revision E.01, Gaussian, Inc., Wallingford, CT, 2004.
4. (a) D. R. Salahub and M. C. Zerner, *The Challenge of d and f Electrons*, ACS, Washington, D.C., 1989; (b) R. G. Parr and W. Yang, *Density Functional Theory of Atoms and Molecules*, Oxford University Press, Oxford, UK, 1989; (c) W. Kohn and L. J. Sham, *Phys. Rev.*, 1965, **140**, A1133-A1138; (d) P. Hohenberg and W. Kohn, *Phys. Rev.*, 1964, **136**, B864-B871.

5. (a) R. E. Stratmann, G. E. Scuseria and M. Frisch, *J. Chem. Phys.*, 1998, **109**, 8218-8224; (b) M. E. Casida, C. Jamoroski, K. C. Casida and D. R. Salahub, *J. Chem. Phys.*, 1998, **108**, 4439-4449; (c) R. Bauernschmitt and R. Ahlrichs, *Chem. Phys. Lett.*, 1996, **256**, 454-464.
6. (a) A. D. Becke, *J. Chem. Phys.*, 1993, **98**, 5648-5652; (b) B. Miehlich, A. Savin, H. Stoll and H. Preuss, *Chem. Phys. Lett.*, 1989, **157**, 200-206; (c) C. Lee, W. Yang and R. G. Parr, *Phys. Rev. B*, 1988, **37**, 785-789.
7. P. Pulay, *J. Comput. Chem.*, 1982, **3**, 556-560.
8. H. B. Schlegel and J. J. McDouall, in *Computational Advances in Organic Chemistry*, C. Ogretir and I. G. Csizmadia, Kluwer Academic, Ed. The Netherlands, 1991, 167.
9. (a) P. J. Hay and W. R. Wadt, *J. Chem. Phys.*, 1985, **82**, 270-283; (b) W. R. Wadt and P. J. Hay, *J. Chem. Phys.*, 1985, **82**, 284-298; (c) P. J. Hay and W. R. Wadt, *J. Chem. Phys.*, 1985, **82**, 299-310.
10. (a) V. A. Rassolov, M. A. Ratner, J. A. Pople, P. C. Redfern, L. A. Curtiss, *J. Comp. Chem.*, 2001, **22**, 976-984; (b) M. M. Francl, W. J. Pietro, W. J. Hehre, J. S. Binkley, D. J. DeFrees, J. A. Pople, M. S. Gordon, *J. Chem. Phys.*, 1982, **77**, 3654-3665; (c) P. C. Hariharan, J. A. Pople, *Mol. Phys.* 1974, **27**, 209-214; (d) P. C. Hariharan, J. A. Pople, *Theo. Chim. Acta.*, 1973, **28**, 213-222; (e) W. J. Hehre, R. Ditchfield, J. A. Pople, *J. Chem. Phys.*, 1972, **56**, 2257-2261.
11. (a) T. Clark, J. Chandrasekhar, G. W. Spitznagel and P. V. R. Schleyer, *J. Comput. Chem.*, 1983, **4**, 294-301; (b) P. C. Hariharan and J. A. Pople, *Theor. Chim. Acta*, 1973, **28**, 213-222.
12. N. M. O'Boyle, A. L. Tenderholt, K. M. Langner, *J. Comp. Chem.*, 2008, **29**, 839-845.
13. (a) M. Cossi, N. Rega, G. Scalmani, V. Barone, *J. Comput. Chem.*, 2003, **24**, 669-681; (b) V. Barone, M. Cossi, *J. Phys. Chem. A.*, 1998, **102**, 1995-2001.